heat transfer in helically coiled tubes, *A.I.Ch.E. Jl* **17**, 1114–1122 (1971).
2. J. M. Tarbell and M. R. Samuels, Momentum and heat transfer in helical coils, *Chem. Engng J.* **5**, 117–127 (1973).
3. S. V. Patankar, V. S. Pratap and D. B. Spalding, Prediction of laminar flow and heat transfer in helically coiled pipes, *J. Fluid Mech.* **62**, 539–551 (1974).
4. M. Akiyama and K. C. Cheng, Laminar forced convection in the thermal entrance region of curved pipes with uniform wall temperature, *Can. J. Chem. Engng* **52**, 234–240 (1974).
5. L. A. M. Janssen and C. J. Hoogendoorn, Laminar convective heat transfer in helical coiled tubes, *Int. J. Heat Mass Transfer* **21**, 1197–1206 (1978).
6. N. Acharya, Experimental and numerical investigation of heat transfer enhancement in coiled tubes by chaotic mixing, Ph.D. Dissertation, University of Notre Dame, Notre Dame, Indiana (1992).
7. F. P. Incropera and D. P. DeWitt, *Fundamentals of Heat and Mass Transfer* (3rd Edn), p. 181. Wiley, New York (1990).
8. Y. Mori and W. Nakayama, Study on forced convective heat transfer in curved pipes (1st report, Laminar region), *Int. J. Heat Mass Transfer* **8**, 67–82 (1965).

Int. J. Heat Mass Transfer. Vol. 37, No. 2, pp. 340–343, 1994
Printed in Great Britain
0017-9310/94 $6.00+0.00

Effect of wall conduction on melting in an enclosure heated at constant rate

YUWEN ZHANG and ZHONGQI CHEN
Department of Power Machinery Engineering, Xi'an Jiaotong University, Xi'an 710049, China

(*Received* 21 *May* 1993 *and in final form* 8 *July* 1993)

1. INTRODUCTION

SOLID–LIQUID phase change phenomena exist widely in nature and industrial processes such as freezing of water and melting of ice, thermal energy storage, casting and metallurgical process, cryogenic preservation of blood and biomaterials, etc. Many typical applications of heat transfer in phase change involve convection in the liquid phase [1]. Recently, boundary layer theory has been adopted to solve the process of natural convection dominated melting. For example, the analytical solution for the melting process in a rectangular enclosure isothermally heated from one of its vertical walls was obtained by Bejan [2].

A series of laboratory experimental results and a compact boundary layer analysis were reported by Zhang and Bejan [3]. In their experiments, the wall heated at constant rate is made of aluminum and heated by eight uniformly spaced strip heaters. The temperature distribution along the two differentially heated vertical walls was measured by means of thermocouples positioned at four altitudes in the vertical mid-plane of the apparatus, and one of their typical measured wall temperatures is quoted in Fig. 1. In their theoretical analysis, the longitudinal conduction along the heated wall was not taken into account, this led to the 100% overprediction of the temperature gradient along the heated wall in the convection regime as illustrated in Fig. 4.

2. PHYSICAL MODEL AND MATHEMATICAL FORMULATION

The physical model adopted is shown as Fig. 2. The heated wall is made of aluminum with thickness w. The wall temperature is uniform as indicated in ref. [3] and rises linearly with time, which corresponds to the melting regime that is ruled by pure conduction; and then reaches a plateau in the convection melting regime. Quasi-steady state is said to be reached after the wall temperatures remain unchanged, all the heat supplied then is used to melt the solid phase change material (n-octadecane was used in ref. [3]). We assume that quasi-steady state is reached; the initial temperature of the solid phase in the enclosure is uniform and equal to the melting point T_m, i.e. no subcooling exists. The equations of the cold boundary layer, warm boundary layer and the core region and their corresponding boundary conditions were reported by Zhang and Bejan as follows [2, 3].

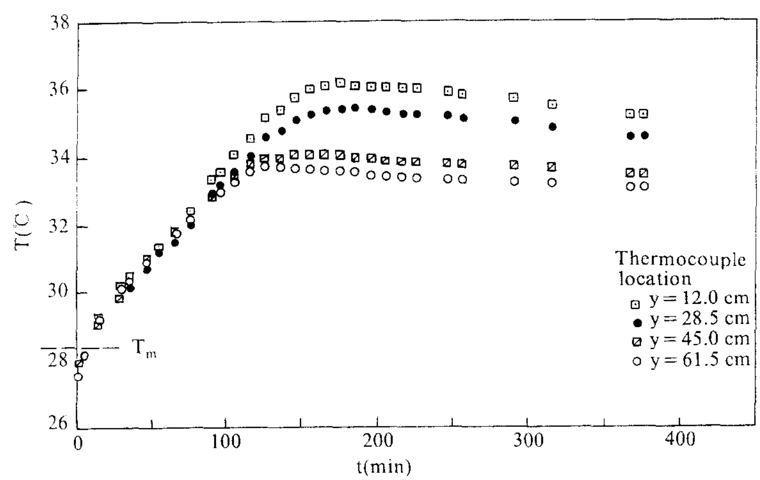

FIG. 1. The history of the temperature distribution along the heated plate [3].

NOMENCLATURE

c_p	specific heat
g	gravitational acceleration
H, L	height and width of enclosure
h_m	latent heat
k	thermal conductivity
K	dimensionless thermal conductivity
q	heat flux
Ra	Rayleigh number
Ste	Stefan number
T	temperature
w	thickness of heated wall
y	vertical coordinate
Y	dimensionless vertical coordinate.

Greek symbols

α	thermal diffusivity of the liquid
β	volumetric thermal expansion coefficient of the liquid
δ	thickness of the cold boundary layer
Δ	dimensionless thickness of the cold boundary layer
θ	dimensionless temperature
λ	thickness of the warm boundary layer
Λ	dimensionless thickness of the warm boundary layer
ν	kinematic viscosity
ρ	density.

Subscripts

c	liquid core
m	melting
w	wall.

The cold boundary layer

$$\frac{2k(T_c-T_m)^2}{\rho h_m \delta}+\frac{g\beta(T_c-T_m)}{36\nu}\frac{d}{dy}[\delta^3(T_c-T_m)] -\frac{g\beta}{60\nu}\frac{d}{dy}[\delta^3(T_c-T_m)^2] = -2\alpha\frac{(T_c-T_m)}{\delta}, \quad (1)$$

$$\delta(H) = 0. \quad (2)$$

The warm boundary layer

$$\frac{g\beta}{90\nu}\frac{d}{dy}[(T_w-T_c)^2\lambda^3]+\frac{g\beta}{36\nu}(T_w-T_c)\lambda^3\frac{dT_c}{dy} = 2\alpha\frac{T_w-T_c}{\lambda}, \quad (3)$$

$$\lambda(0) = 0. \quad (4)$$

The core region

$$\delta^3(T_c-T_m) = (T_w-T_c)\lambda^3, \quad (5)$$

$$T_c(0) = 0, \quad (6)$$

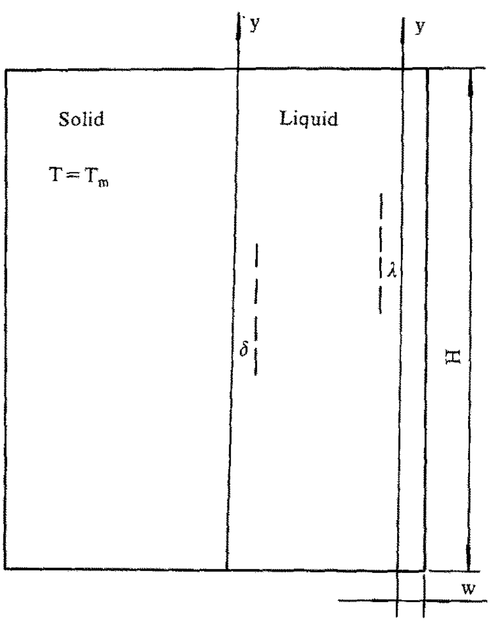

FIG. 2. Physical model of the analysis.

$$T_c(H) = T_w(H). \quad (7)$$

The longitudinal conduction of the aluminum plate can be simplified as a one-dimensional steady-state conduction, i.e.

$$\frac{d}{dy}\left(k_w w\frac{dT_w}{dy}\right)+Q = 0, \quad (8)$$

where Q is the difference between the amount of heat provided by the strip heaters q and that transferred to the phase change materials through the left side of the heated wall, it can be expressed as

$$Q = q-\frac{2k(T_w-T_c)}{\lambda}. \quad (9)$$

The top and bottom of the heated wall are adiabatic, so the boundary condition for equation (8) is

$$\frac{dT_w}{dy} = 0, \quad \text{at} \quad y = 0 \quad \text{and} \quad y = H. \quad (10)$$

3. SOLUTIONS

Defining the following dimensionless variables

$$Ste_* = \frac{c_p(qH/k)}{h_m}, \quad Ra = \frac{g\beta(qH/k)H^3}{\nu a}, \quad Ste = Ste_* Ra^{-1/5}$$

$$Y = \frac{y}{H}, \quad \Delta = \frac{\delta}{H}Ra^{1/5}, \quad \Lambda = \frac{\lambda}{H}Ra^{1/5}, \quad \theta = \frac{(T-T_m)}{qH/k}Ra^{1/5} \quad (11)$$

we get the dimensionless ordinary differential equations

$$2Ste\frac{\theta_c^2}{\Delta}+\frac{\theta_c}{36}\frac{d}{dY}(\Delta^3\theta_c)-\frac{1}{60}\frac{d}{dy}(\Delta^3\theta_c^2) = -2\frac{\theta_c}{\Delta}, \quad (12)$$

$$\frac{1}{90}\frac{d}{dY}[(\theta_w-\theta_c)^2\Lambda^3]+\frac{1}{36}(\theta_w-\theta_c)\Lambda^3\frac{d\theta_c}{dY} = 2\frac{\theta_w-\theta_c}{\Lambda}, \quad (13)$$

$$\Delta^3\theta_c = (\theta_w-\theta_c)\Lambda^3, \quad (14)$$

$$\frac{d}{dY}\left(\frac{k_w}{k}W\frac{d\theta_w}{dY}\right)+Q^* = 0, \quad (15)$$

$$Q^* = Ra^{1/5}\left[1-\frac{2(\theta_w-\theta_c)}{\Lambda}\right], \quad (16)$$

and their corresponding boundary conditions are

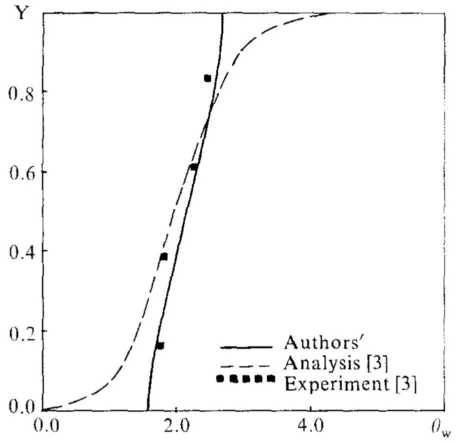

FIG. 3. Wall temperature distributions [3].

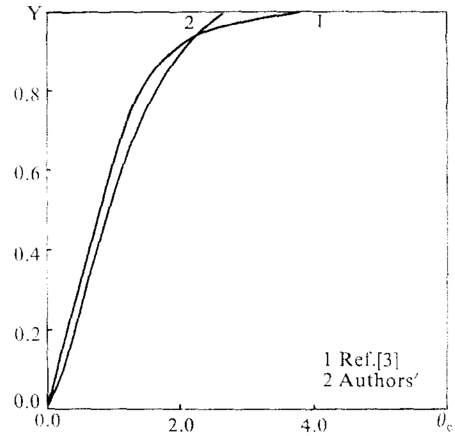

FIG. 5. Comparison of core temperature.

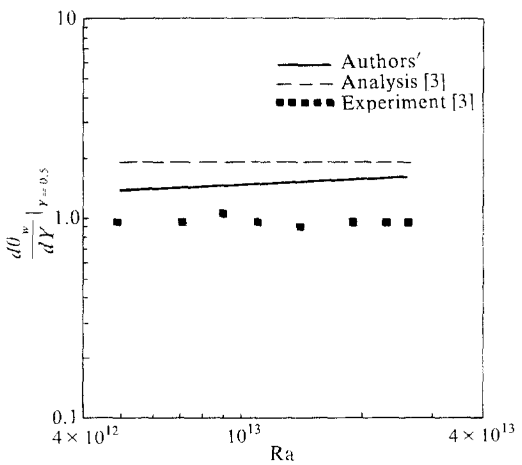

FIG. 4. Wall temperature gradient at $Y = 0.5$.

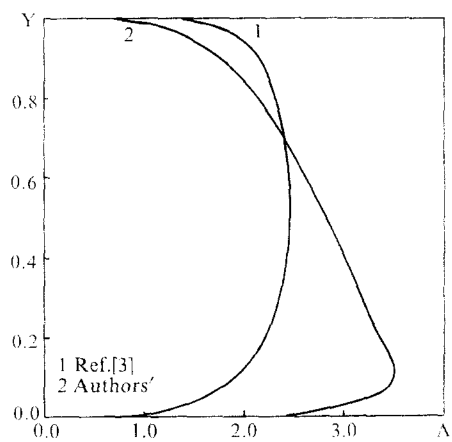

FIG. 6. Thickness of warm boundary layer.

$$\left.\begin{array}{l} Y = 0: \quad \Lambda = 0, \quad \theta_c = 0, \quad \dfrac{d\theta_w}{dY} = 0 \\ Y = 1: \quad \Delta = 0, \quad \theta_c = \theta_w, \quad \dfrac{d\theta_w}{dY} = 0 \end{array}\right\}. \tag{17}$$

The above differential equations are solved numerically. The number of nodal points along the height is $N = 2000$ in the calculation. The convergence criterion used for both θ_c and θ_w is 10^{-9}. No relaxation is needed during iteration.

4. RESULTS AND DISCUSSIONS

The agreement between experimental and predicted wall temperature is greatly improved by taking the wall conduction into account as shown in Fig. 3. It can be understood that the wall temperature tends to be more uniform because of the longitudinal conduction. The agreement between experiment and analysis is also improved for the temperature gradients at the midpoint of the heated aluminum plate as demonstrated in Fig. 4, the discrepancies still existing may be attributed to the oversimplification of the one-dimensional conduction assumption.

Figure 5 shows the comparison of the core temperature distributions for $Ste = 0$ to Zhang and Bejan's prediction. The wall conduction leads the core temperature to be more uniform. But the effect of wall conduction on the core temperature is smaller than that on the wall temperature.

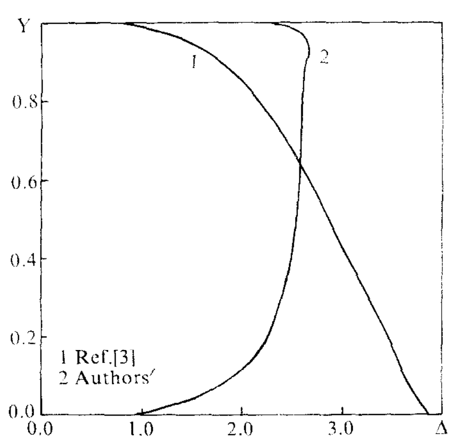

FIG. 7. Thickness of cold boundary layer.

Thickness of the warm boundary layer for $Ste = 0$ is shown in Fig. 6. The thickness increases in the lower part of the plate and the reverse is true in the upper part as compared to Zhang and Bejan's prediction. As to the thickness of the cold boundary layer, i.e. the boundary layer along the solid–liquid interface, opposite variations were revealed as shown in Fig. 7.

Acknowledgement—Financial support by The Chinese National Natural Science Foundation under Grant No. 59276260 is greatly appreciated.

REFERENCES

1. R. Viskanta, Natural convection melting and solidification. In *Natural Convection: Fundamentals and Applications* (Edited by S. Kakac, W. Aung and R. Viskanta). Hemisphere, New York (1985).
2. A. Bejan, Analysis of melting by natural convection in an enclosure, *Int. J. Heat Fluid Flow* **10**(3), 245–252 (1989).
3. Z. Zhang and A. Bejan, Melting in an enclosure heated at constant rate, *Int. J. Heat Mass Transfer* **32**, 1063–1076 (1989).